water

MDPI

Article

Conversion of Blue Water into Green Water for Improving Utilization Ratio of Water Resources in Degraded Karst Areas

Ke Chen [1,2], Shengtian Yang [3,*], Changsen Zhao [1,2], Zongli Li [4], Ya Luo [5], Zhiwei Wang [1,2], Xiaolin Liu [1,2], Yabing Guan [1,2], Juan Bai [1,2], Qiuwen Zhou [5] and Xinyi Yu [1,2]

1 State Key Laboratory of Remote Sensing Science, School of Geography, Beijing Normal University, No.19, Xinjiekouwai Street, Haidian District, Beijing 100875, China; chenkebj2000@sina.com (K.C.); zhaochangsen@bnu.edu.cn (C.Z.); wangzhiweisci@gmail.com (Z.W.); liuxiaolin@163.com (X.L.); guanyabing@mail.bnu.edu.cn (Y.G.); baijuanaction@163.com (J.B.); yuxy0106@sina.com (X.Y.)

2 Beijing Key Laboratory for Remote Sensing of Environment and Digital Cities, Haidian District, Beijing 100875, China

3 College of Water Sciences, Beijing Normal University, No.19, Xinjiekouwai Street, Haidian District, Beijing 100875, China

4 China Renewable Energy Engineering Institute, Xicheng District, Beijing 100120, China; lizongli@giwp.org.cn

5 School of Geographic and Environmental Sciences, Guizhou Normal University, Guiyang 550001, China; luoya2002@163.com (Y.L.); zouqiuwen@163.com (Q.Z.)

* Correspondence: yangshengtian@bnu.edu.cn; Tel.: +86-10-5880-5034

Academic Editor: Athanasios Loukas

Received: 24 September 2016; Accepted: 28 November 2016; Published: 5 December 2016

Abstract: Vegetation deterioration and soil loss are the main causes of more precipitation leakages and surface water shortages in degraded karst areas. In order to improve the utilization of water resources in such regions, water storage engineering has been considered; however, site selection and cost associated with the special karstic geological structure have made this difficult. According to the principle of the Soil Plant Atmosphere Continuum, increasing both vegetation cover and soil thickness would change water cycle process, resulting in a transformation from leaked blue water (liquid form) into green water (gas or saturated water form) for terrestrial plant ecosystems, thereby improving the utilization of water resources. Using the Soil Vegetation Atmosphere Transfer model and the geographical distributed approach, this study simulated the conversion from leaked blue water (leakage) into green water in the environs of Guiyang, a typical degraded karst area. The primary results were as follows: (1) Green water in the area accounted for <50% of precipitation, well below the world average of 65%; (2) Vegetation growth played an important role in converting leakage into green water; however, once it increased to 56%, its contribution to reducing leakage decreased sharply; (3) Increasing soil thickness by 20 cm converted the leakage considerably. The order of leakage reduction under different precipitation scenarios was dry year > normal year > rainy year. Thus, increased soil thickness was shown effective in improving the utilization ratio of water resources and in raising the amount of plant ecological water use; (4) The transformation of blue water into green water, which avoids constructions of hydraulic engineering, could provide an alternative solution for the improvement of the utilization of water resources in degraded karst area. Although there are inevitable uncertainties in simulation process, it has important significance for overcoming similar problems.

Keywords: degraded karst areas; blue water; green water; leakage; Guiyang; SPAC; SVAT; conversion

1. Introduction

"Green water", which is a critical concept in ecological hydrology research, was proposed initially in 1995 by Malin Falkenmark, a hydrologist with the Stockholm International Water Institute [1]. She distinguished two types of precipitation: green water, which is stored in the soil and plants and circulates within the terrestrial plant ecosystem, and blue water, which supplies aquatic ecosystems and human consumption (Figure 1). It has been established that about 65% of global precipitation is returned to the atmosphere via green water in the form of evapotranspiration from forests, grassland, wetland, and farmland, whereas only about 35% of global precipitation is retained in the form of blue water in rivers, lakes, and aquifers [2,3]. Stewart et al. (2015) [4] argued that green water was often <30% of the precipitation in arid regions, and >65% in more humid areas. Based on previous research, Falkenmark and Rockstrom [5] further divided green water into green water flow and green water storage from the perspective of the hydrological cycle. They indicated that green water is a dynamic conversional process, i.e., when green water is consumed, it is also replenished. Green water circulation objectively reflects the water consumption process of the natural "soil-vegetation" ecological system [6]. Green water provides the necessary growth conditions for land plants and thus, it is very important for terrestrial plant ecosystem. Recently, Hoekstra et al. (2011) [7] pointed out clearly that blue water included fresh surface and groundwater, i.e., the freshwater in lakes, rivers and aquifers; and green water included precipitation on land that did not run off or recharge the groundwater, but was stored in the soil or temporarily stays on the top of the soil or vegetation. Later, Launiainen et al. (2014) [8] and Quinteiro et al. (2015) [9] further confirmed the new statement of blue water and green water proposed by Hoekstra et al. which indicated specifically the scope of blue water and green water. The distinction between blue water and green water has broadened the scope of the traditional view of water resources, and it has prompted the scientific community to rethink the concept of water resources, as well as the ecological function of water [10]. Given the current threat of globally reduced water resources, the concept of green water could be used to identify more clearly the function and scope of ecological water, and to provide a theoretical foundation for the protection of soil and water resources. The objective of "water conservation" in the field of water and soil conservation is to protect green water resources [11].

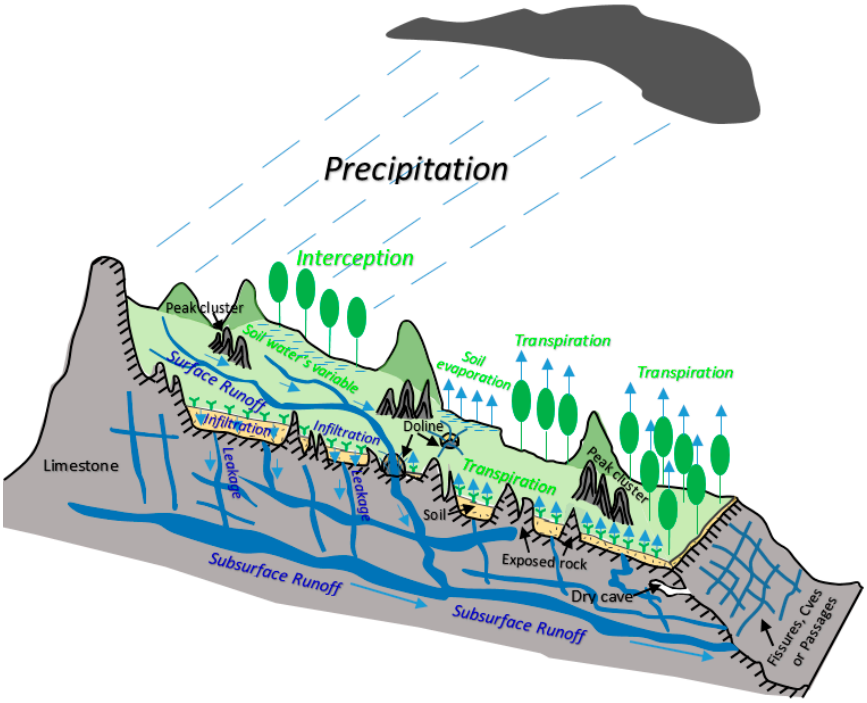

Figure 1. Processes associated with blue water and green water in degraded karst area. Note: Blue arrows imply the direction of water flow. Blue font indicates blue water and green font indicates green water.

In karst regions, the unique karst geological structures of the area result in considerable soil and water loss [12,13] because karst limestone facilitates leakage and erosion, allowing precipitation to escape in the form of leakage (blue water) through its underground drainage system [14–16], which is the main cause of local shortages of surface water [17,18]. Specific to degraded karst areas where rocky desertification is generally distributed [19], the degradation of vegetation and thin soil cover further increase precipitation leakage. This "leaked" precipitation often becomes unavailable underground blue water that contributes to the low utilization ratio of local water resources. As described above, precipitation comprises two parts: green water, which participates in vegetation evaporation and blue water, which flows off in the form of outflow. If a large amount of precipitation were to be lost in the form of leakage (blue water), the green water that originally should have been available to participate in evaporation would inevitably be reduced.

Historically, destruction of the ecological environment has been the direct cause of worsening rocky desertification and increased surface water shortages in degraded karst areas [16,20–22]. Gams and Gabrovec (1999) [23] discovered that anthropogenic activity on the Kras Plateau in Slovenia had caused great damage to the forest since last centuries B.C., which resulted in large area of bare rock outcropped on the ground surface. In the European Mediterranean basin, rocky desertification has also been accelerated by the destruction of forests for land reclamation [24]. In China, deforestation had brought about large-scale rocky desertification in karst regions during the period of the "Great Leap Forward" (1958–1961). According to statistics, in Guizhou Province alone where there are large number of karst regions [19,25], the area of rocky desertification expanded considerably by 3.76 times from 1970 to 2005 [26]. Based on a study in Guizhou Province, Wang et al. (2004) [27] found that vegetation deterioration, soil loss, and outcropping of rocks led to serious water shortages (local permeability coefficients are commonly 0.3–0.6). It has been established that the huge losses of water via leakage makes most of Guizhou Province a "karstic drought area under the condition of hot and humid climate" [28]. Jiang et al. (2014) [26] indicated that rocky desertification resulted in fewer plants able to store surface water, therefore, there is considerable leakages and drought in degraded karst areas where topsoil is thin and vegetation coverage scant. Huang et al. (2008) [29] found that huge losses of precipitation via leakage resulted in frequent drought and seriously affected the normal growth of local crops and vegetation in degraded karst areas. It is clear that rapid leakage of precipitation resulting from the degradation of vegetation and soil is the fundamental reason for the aggravation of surface water shortages in degraded karst areas. Therefore, if there were appropriate measures to be taken to improve the utilization ratio of precipitation, it would have a positive impact on the ecological and economic development of degraded karst areas.

In recent years, there has been increased research to address the problems of surface water shortages and to improve the utilization ratio of water resource in degraded karst areas. Many researchers believe that the shortage of surface water in degraded karst areas is an engineering problem that can be overcome by constructions, such as precipitation collection projects, or the extraction of water from subterranean rivers and underground reservoirs [14,30–32]. However, experience has shown that the construction of water storage engineering projects in karst areas is very expensive [14,33], and the permeability of the limestone makes the selection of appropriate engineering sites a huge problem [34–36]. Moreover, Mohammadi et al. (2007) [37] and Guo et al. (2013) [16] found out that reservoirs in karst areas commonly suffered serious problem of leakage. Some researchers have explored solutions from the perspective of ecological water use. For example, Su (2006) [38] suggested increasing the volume of ecological water to maintain the health of ecological systems. Li et al. (2011) [39] attempted to calculate the ecological water requirements and shortages associated with the cultivation of Chinese prickly ash (a major economic crop) by simulating the evaporation and transpiration in the southwest of Guizhou Province. Yang et al. (2009) [40] proposed a quantitative simulation model for ecological water requirements in central Guizhou Province and concluded that the order of ecological water requirements of different vegetation type was: farmland > bushland > forestland > grassland. Zuo et al. (2014) [41] established an index system to evaluate quantitatively the ecological carrying

capacity of water resources in Guizhou Province during 2007–2010, arguing that the carrying capacity was not stable. By establishing the "water resources allocation" model and calculations, Song et al. (2015) [42] believed that a large number of water diversion from the west part of Guizhou province to its central part would be beneficial to the ecological restoration in central of Guizhou. Tong et al. (2016) [25] argued that limited by a low water use efficiency, the ecological recovery effect in southwest of China was questionable. Although these researchers performed thorough analyses of water resource utilization from the perspective of ecological restoration in degraded karst areas, and some even calculated the ecological water volume for evaluation and analysis via numerical simulation, they did not clarify how to improve the ecological water share.

These studies above analyzed the reasons for and the effects of surface water shortages in degraded karst areas from the perspectives of engineering and ecological water use. However, a specific and feasible solution to the water shortage in degraded karst areas still need to explore. Furthermore, there have been few in-depth analyses from the perspective of the conversion of blue water into green water. In degraded karst areas, where vegetation coverage is scant and the soil is thin, an investigation of blue water and green water would assist in the exploration of feasible methods through which poorly accessible leaked blue water could be transformed into useful green water for ecological and economic purposes, thereby promoting local sustainable development.

In this study, in order to explore the way to convert the unavailable leaked blue water into green water for improving local water resources utilization, the spatial distributions of blue water and green water, especially leaked precipitation in a typical degraded karst area (i.e., the environs of Guiyang) from 2003 to 2013 were simulated by the Soil Vegetation Atmosphere Transfer (SVAT) model. Based on the obtained results, the corresponding transformation measures by which the leaked blue water was converted into green water were analyzed and proposed.

2. Study Area and Data

2.1. Study Area

Guiyang as the provincial capital of Guizhou province, is located at 26°11′–27°22′ N, 106°07′–107°17′ E, which is in the central of Guizhou province and on the eastern slope of the Yunnan–Guizhou plateau, China. Guiyang covers an area of 8034 km^2, of which 85% comprises karst landforms [43]. Guiyang is situated in a subtropical humid monsoon climate zone, where less than approximately 1/10 of the local land area is used as typical rain-fed agricultural farmland. The selected study area (about 7495 km^2) is the environs of Guiyang (Figure 2), which lies at the heart of karst landforms in China. Because of the deforestation history, the planted forest occupied the main area of local forestland which was about 704 km^2, and the grassland was about 153 km^2 [44]. The karst coverage ratio exceeds 80% (Gao et al., 2016) [45], and about 37% of local area is affected by soil erosion—the soil layer has become increasingly thin and stony [27,46].

As a typical degraded karst area in southwest China, Guiyang has 98 rivers that are more than 10-km long and annual average precipitation of 1120 mm; however, the high level of karstic permeability results in considerable leakages of precipitation [47], which causes the utilization ratio of local water resources is only about 20.5% [48]. Given the current level of technical competence that makes it difficult to extract leaked blue water, it is especially important to take measures to convert the leaked blue water into green water for raising the utilization ratio of local water resources.

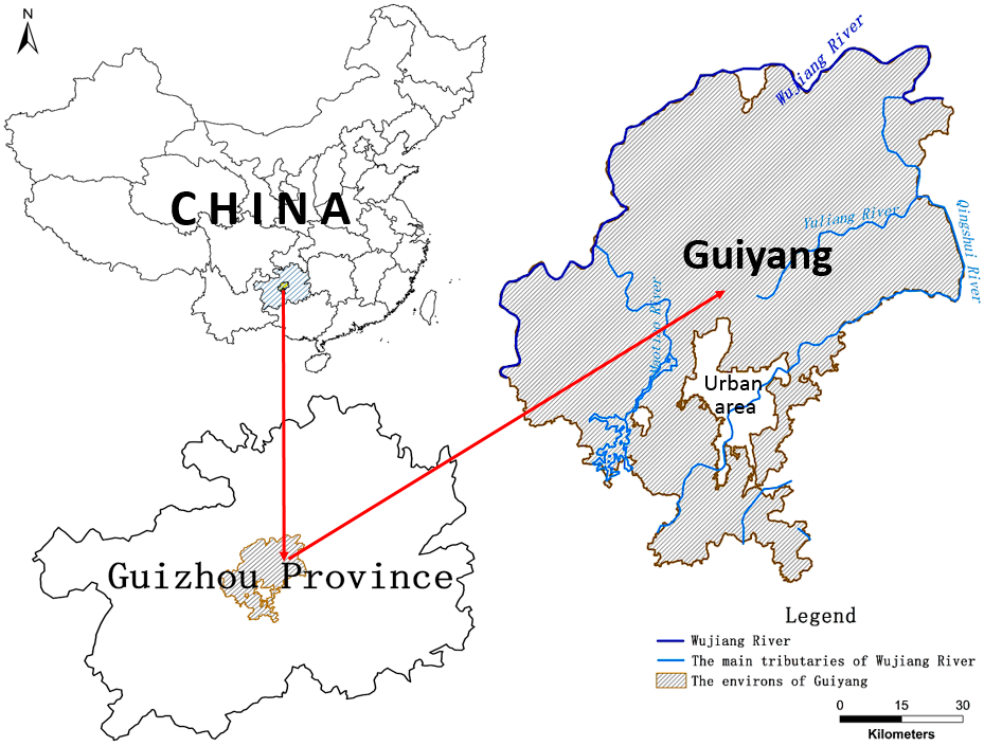

Figure 2. Location of Guiyang, Southwest China.

2.2. Data

The data used for the calculation of evapotranspiration and soil water transport comprised meteorological and basic geographical data [49,50]. Meteorological data mainly included land surface temperature (LST), surface albedo, the 31st/32nd band emissivity of MODIS, sunrise time and sunset time, the instantaneous temperature (Tair) and daily precipitation. Basic geographical data mainly included digital elevation model (DEM), scope of longitude/latitude, leaf area index (LAI), vegetation coverage (Landcover), soil type, land use and soil thickness. Meteorological data combined with the data of LAI, vegetation coverage and land use were used to simulate vegetation transpiration and interception of precipitation process. Meteorological data combined with the data of soil texture, land use and soil thickness were used to simulate soil evaporation, infiltration and leakage process. The data contents and acquisition methods are shown in Table 1.

In Table 1, the data of digital elevation (DEM) was obtained from public free platforms (e.g., Advanced Spaceborne Theemal Emission and Reflection Radiometer Global Digital Elevation Model net (ASTER GDEM)) [51], the data of instantaneous temperature and precipitation measurements were obtained from public free platforms (e.g., the Portal of Chinese Science and Technology Resource net (PCSTR)) [52]. The data of LAI, vegetation coverage, land use, the 31st/32nd band emissivity of MODIS and surface radiation were obtained from MODIS remote sensing products platform (e.g., NASA's Earch Observing System Data and Information System net) [53]. In addition, sunrise/sunset time were calculated based on location and date, soil type data were obtained from Harmonized World Soil Database (HWSD), the data of soil thickness were determined mainly based on field investigation.

Based on the remote sensing data available and the requirements of the calculations, the spatial resolution of the basic geospatial data was 1 km, the time step of the simulation was one year. In general, the longer the data's time spans, the more conductive to analyzing the change regular. Given partial atmospheric data was lack before 2003 year, and some data after 2013 were not issued when this study started, 2003 year was set as the initial year and 2013 year was set as the current year.

Table 1. Initial input data of the SVAT model.

Data Name	Data Contents	Unit	Acquisition Methods
DEM_0	Digital elevation model	m	ASTER GDEM
Longitude_0	Scope of longitude	°	Spatial interpolation
Latitude_0	Scope of latitude	°	Spatial interpolation
Albedo_date	Surface albedo	-	MODIS
Emis31_date	The 31st band emissivity of MODIS	-	MODIS
Emis32_date	The 32nd band emissivity of MODIS	-	MODIS
LST_date	Land surface temperature	K	MODIS
T_rise_date	Sunrise time	h	Calculation based on location and date
T_set_date	Sunset time	h	Calculation based on location and date
Tair_instant_date	The instantaneous temperature	K	PCSTR (Kriging interpolation)
Lai_date	Leaf area index	-	MODIS
Landcover_date	Vegetation coverage	-	Equations (12)–(14)
Precipitation_date	Daily precipitation	mm	PCSTR (Kriging interpolation)
Soil_Type_0	Soil type	-	Harmonized World Soil Database
Land_Type_0	Land use	-	Drawing based on MODIS
Model_init_txt_0	Soil thickness	-	Field investigation

Notes: When the simulation was conducted, these data whose filename suffix was "date" would be calculated by the day, for example, Lai_001 implied the Lai's value of the first day in a year and Lai_365 implied the Lai's value of the 365th day in a year. Those data whose filename suffix was "0" would be put into the SVAT model only one time for one year's calculation, such as DEM_0, Longitude_0, Land_Type_0 and so on.

3. Methodology

3.1. Theoretical Basis

The principle of the Soil Plant Atmosphere Continuum (SPAC), which recognizes the evapotranspiration process of plants as an important link [54–56], provides the theoretical basis for the study of water transmission from blue water into green water. The SPAC energy and moisture calculation process is primarily concerned with three major links: evaporation, vegetation interception, and soil moisture migration [50,57], which entirely comprises the cycle process of green water, as shown in Figure 3. According to the principle of SPAC, the three main factors that affect the water cycle are soil, vegetation, and atmospheric precipitation. Given atmospheric precipitation is uncontrolled, the present adjustment objects of conversion from blue water into green water are only soil (thickness) and vegetation (coverage).

According to the SPAC principle, the water vapor from plant surfaces into atmosphere (vegetation transpiration) is green water, and part of the plant surfaces' water vapor comes from the vegetation interception of precipitation. Assuming that the precipitation of a region is unchanged, if the vegetation coverage was increased, vegetation transpiration (green water) would be increased too, according to the principle of water balance, when much precipitation is intercepted by plant surfaces, runoff including leakage (blue water) would be decreased. In addition, another part of plant surfaces' water vapor comes from soil saturated water (green water) through plant roots, if the soil thickness is increased, the storage capacity of soil water would be strengthened, much soil saturated water would be conveyed for vegetation transpiration, and soil evaporation (green water) would be increased too, while, at the same time, runoff including leakage (blue water) would be decreased. This is the whole conversion process of blue water into green water.

The SPAC principle has been used and verified extensively in earlier research [58–61]. Recently, Gao et al. (2015) [62] testified that the SPAC principle is not only suitable for arid and semiarid areas but also for the relatively humid karst rocky desertification area in the southwest of China.

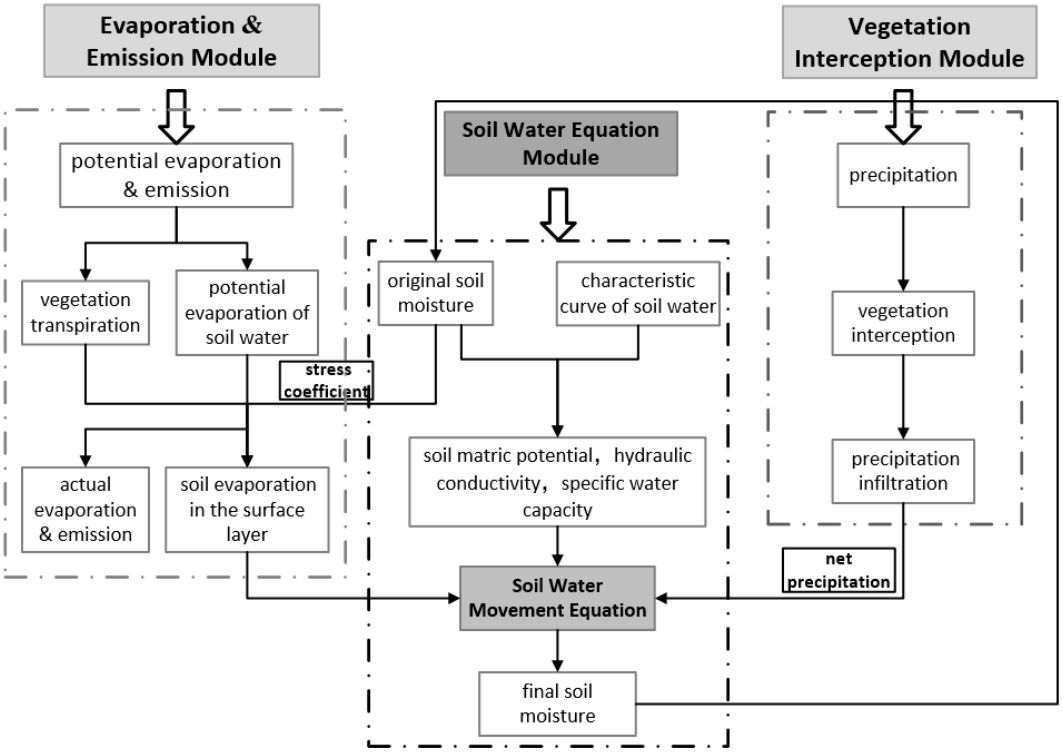

Figure 3. Soil Plant Atmosphere Continuum energy and moisture calculation process (Yang et al., 2015 [50]).

The SVAT model, based on the SPAC principle, is a model that has been used for studies of karst rocky desertification regions in Guizhou Province, providing a wealth of useful research fruits. Wang et al. (2008) [63] used the SVAT model in conjunction with remotely sensed data to simulate the consumption utility difference of green water in Longli County (Guizhou Province), and they found that the consumption of green water per unit area in forest, grassland, scrubland, and farmland was 423.0, 344.2, 386.7, and 407.5 mm, respectively. Yang et al. (2009) [40] used the SVAT model, multiple sources, and temporal images to simulate the water cycle process of surface soil evaporation, vegetation interception, plant transpiration, and soil water storage and they verified the accuracy of the results. In 2010, Wen et al. (2010) [6] adopted the SVAT model to simulate the cycle of green water in central Guizhou Province on the regional scale, believing that: "As the karst ecological restoration and vegetation type change, more precipitation shall be converted into green water, i.e., ecological water use". Based on an analysis of long-term field observations in Longli County, Yang (2014) [64] argued that the green water resource is an important restrictive factor in local ecological restoration. In addition, By research in Guizhou, Gao et al. (2013) [65] found that vegetation recovery was helpful to increase precipitation, and thus increase the amount of evaporation in karst areas. Li et al. (2014) [66] and Gao et al. (2016) [45] believed that potential evapotranspiration was an important integral component of hydrological cycle, and argued that the potential evapotranspiration of Guizhou presented a trend of decrease in the past 50 years. Therefore, it is evident that the importance of the transformation between blue water and green water, and the attribution of green water to a local terrestrial plant ecosystem, has been acknowledged quantitatively through the application of the SVAT model to the degraded karst area of Guizhou Province.

3.2. *Assessment Formulas of Blue Water and Green Water*

Based on the SPAC theory, using the SVAT model, and relying on the EcoHAT ecological hydrology system program developed by Beijing Normal University, the amount of soil water movement can

be derived by simulating the variation processes of blue water and green water in vegetation and soil [67,68]. Then, as a component of soil water movement, the leakage volume can be determined. The computation formulas on which the SVAT model is based are as follows.

3.2.1. Evapotranspiration Calculation

The formula [69] can be expressed as:

$$ET_P = \alpha \left(\frac{Rn - G}{\lambda} \right) \left(\frac{\Delta}{\Delta + \gamma} \right) \tag{1}$$

where ET_P is the potential evapotranspiration (unit: mm), α is the Priestley–Taylor coefficient, Rn is the net radiation of the land surface (unit: W/m^2), G is the soil heat flux (unit: W/m^2), λ is the latent heat of vaporization (unit: MJ/kg), Δ is the slope of the pressure–temperature curve of saturated water (unit: kPa/°C), and γ is the constant value of the psychrometer (unit: kPa/°C). By calculating the evapotranspiration of Duck Pond River watershed, which is close to Guiyang, and according to the comparison of observation data and water balance, Zhao et al. (2011) [70] figured that the value of α in the watershed was 1.16. Priestly–Taylor model with fewer parameters has been widely used in the calculation of potential evapotranspiration [71–73]. The following simulation for evapotranspiration process mainly used the calculation formulas of SVAT model relying on the EcoHAT system [50,67].

$$EP_s = \begin{cases} ET_p \times (1 - 0.43 \times LAI), & LAI \leq 1 \\ ET_p \times exp(-0.4 \times LAI), & 1 < LAI < 3 \\ 0 \quad , & LAI > 3 \end{cases} \tag{2}$$

where EP_s is the potential soil evaporation (unit: mm), ET_P is the potential evapotranspiration (unit: mm), and LAI is the leaf area index.

$$EPS = EP_s \times K_{ss} \tag{3}$$

$$K_{ss} = \begin{cases} 0 \quad , & \theta < \theta_w \\ (\theta - \theta_w) / (\theta_j - \theta_w), & \theta_w < \theta \leq \theta_j \\ 1 \quad , & \theta \geq \theta_j \end{cases} \tag{4}$$

$$\theta_j = \theta_f \times 0.75 \tag{5}$$

where EPS is the actual soil evaporation (unit: mm), EPs is the potential soil evaporation (unit: mm), Kss is the water stress coefficient, θ is the soil moisture content (%), θ_w is the wilting point (%), θ_j is the moisture content at capillary rupture (%), and θ_f is the field capacity (%).

$$EPv = \begin{cases} \frac{ET_p \times LAI}{3}, & 0 \leq LAI \leq 3 \\ ET_P, & LAI > 3 \end{cases} \tag{6}$$

$$EPn = EPv \times RDF \tag{7}$$

$$E - Plant = \sum_{i=1}^{n} EPn \tag{8}$$

$$RDF = \frac{e^{AROOT \times Z_2} - e^{AROOT \times Z_1}}{e^{AROOT \times LR} - 1} \tag{9}$$

$$Rd_i = Rd_{max} \frac{LAI_i}{LAI_{max}} \tag{10}$$

where EPv is the total potential vegetation transpiration (unit: mm); ET_P is the potential evapotranspiration (unit: mm); EPn is the actual vegetation transpiration of the n-th layer's soil (unit: mm), *E-plant* is the total vegetation transpiration (unit: mm); RDF is the root distribution

function; *AROOT* is the parameter of root distribution and its value is 0.1; Z_1 and Z_2, are respectively, the two ends' coordinate in the vertical direction of the n-th layer soil; *LR* is the root depth (unit: m); Rd_i is the root depth at the period of time I (unit: m); LAI_i is the leaf area index at the period of time I; and LAI_{max} is the maximum leaf area index.

3.2.2. Vegetation Intercept Calculation

Here, the formula for the vegetation intercept calculation of Aston (1979) [74] was adopted:

$$S_v = C_v \times S_{max} \times \left(1 - e^{-\eta \frac{P_{cum}}{S_{max}}}\right) \tag{11}$$

$$C_v = 1 - e^{-k \times LAI} \tag{12}$$

$$k = \Omega \times R \tag{13}$$

$$R = 0.5/cos\ \theta_z \tag{14}$$

where S_v is the vegetation intercept (unit: mm), C_v is vegetation coverage, P_{cum} is the cumulative precipitation (unit: mm), S_{max} is the maximum amount of canopy interception (unit: mm), η is a correction coefficient, k is the extinction coefficient associated with the sun light conditions, *LAI* is the leaf area index, θ_z is the solar zenith angle, and Ω is the aggregation index related to land cover types.

The estimation of the greatest quantity of canopy entrapment (S_{max}) and the correction coefficient are based on the leaf area index (*LAI*), the formulas for which are:

$$S_{max} = 0.935 + 0.498 \times LAI - 0.00575 \times LAI^2 \tag{15}$$

$$\eta = 0.046 \times LAI \tag{16}$$

3.2.3. Soil Water Transport Calculation

According to the principle of water balance, the movement of soil water in vertical direction can be simulated, and, thereby, leakage volume is obtained. Vertical soil water movement in one dimension can be described using Richard's Equation [75,76]:

$$C(h)\frac{\partial h}{\partial t} = \frac{\partial}{\partial z}\left[K(h)\left(\frac{\partial h}{\partial z} + 1\right) - S(h)\right] \tag{17}$$

$$\begin{cases} C(h)\frac{\partial h}{\partial t} = \frac{\partial}{\partial z}\left[K(h)\frac{\partial h}{\partial z}\right] - \frac{\partial K(h)}{\partial z} \\ h(z,0) = h_0(z) \quad (0 \le z \le L_z) \\ \left[-K(h)\frac{\partial h}{\partial z} + K(h)\right]_{z=0} = \begin{cases} -E(t) \\ Q(t) \end{cases} \quad (t > 0) \\ h(L_z,t) = h_1(t) \quad (t > 0) \end{cases} \tag{18}$$

where h is the soil water matric potential (i.e., the negative pressure head of the soil water; unit: cm), $C(h)$ is the water capacity (unit: /cm), $C(h) = -d\theta/dh$; $K(h)$ is the unsaturated hydraulic conductivity (unit: cm/min), $E(t)$ is the evaporation's strength of the surface of the soil (unit: cm/min), $Q(t)$ is the intensity of precipitation infiltration (unit: cm/min), z is space coordinate, t is time coordinate, and L_z is vertical soil depth (cm). The value of net precipitation after subtraction of vegetation interception is the upper boundary condition of soil water movement, the portion of infiltrated water passing the lower boundary of the soil is considered to be groundwater (blue water) and is termed leakage.

The value of unsaturated hydraulic conductivity $K(h)$ was obtained according to the following formula:

$$K(h) = \begin{cases} Ks \cdot \exp(a \cdot h), & h < 0 \\ Ks, & h \ge 0 \end{cases} \tag{19}$$

where *Ks* is saturated hydraulic conductivity (the values of different soil textures are in Table 2), and *a* is the fitting parameter.

Table 2. The generalized parameters and saturated hydraulic conductivity (*Ks*).

Soil Texture	P_1	P_2 (cm)	P_3	P_4	*Ks* (cm/min)
Heavy Clay	0.28	70.030	0.66	0.27	0.000006
Clay	0.28	50.159	0.63	0.16	0.00006
Silty Loam	0.31	175.995	0.80	0.11	0.0006
Loam	0.32	186.441	0.86	0.09	0.006
Sandy Loam	0.28	247.682	0.92	0.09	0.06

Notes: Paddy soil and ground objects that are not soil and are classified into heavy clay, whose hydraulic conductivity is the lowest among all these soil types.

The relationship between soil matrix potential and soil moisture content was described by the following formula:

$$W = \begin{cases} \frac{P_1 \times P_2}{P_2 + |h|^{P_3}} + P_4, & h < 0 \\ W_s \quad , & h \geq 0 \end{cases} \tag{20}$$

where W is the soil moisture content; h is the soil matric potential; P_1, P_2, P_3 and P_4 are the generalized parameters; Ws is the saturation moisture content; and $Ws = P_1 + P_4$.

The water storage variation can be figured out based on the soil moisture content, the formula is as:

$$\Delta W = \sum_{i=1} (W_{i+1} - W_i) \tag{21}$$

where ΔW is the water storage variation, and W_i is the water storage at the period of time i.

In addition, according to the principle of water balance, the runoff can be determined using the following formula:

$$R = P - I - T - E - \Delta W \tag{22}$$

where R is the quantity of runoff, P is the quantity of precipitation, I is the quantity of vegetation intercept, T is the quantity of vegetation transpiration, E is the quantity of evaporation from soil, and ΔW is the water storage variation. The units of these variables are mm.

The calculation of soil water transport includes values for vegetation transpiration, vegetation interception, soil evaporation, soil water storage, and leakage. Among these, the leakage not involved in the plant growth process is blue water, whereas all other parameters are green water. In addition, the runoff inferred from the water balance principle is also blue water.

3.3. Key Parameters in the SVAT Model

As a principal embedded model of the EcoHAT system program, the SVAT model has been used for simulations of the evaporation and green water processes by Wang et al. (2008) [63], Wen et al. (2010) [6], and Yang et al. (2014) [64] in an area which is close to Guiyang. Therefore, the SVAT model could be regarded as a pre-established calibration model in this study.

The parameters that would influence the reliability of the calculation results mainly include soil thickness, root depth, soil texture, and soil hydraulic conductivity. According to field investigation and the experiments of Wen et al. (2010) [6] and Yang et al. (2014) [64], the value of soil thickness was identified as 40 cm. The values of root depth were determined based on vegetation type and land use. The values of soil texture and saturated hydraulic conductivity were based on the data validated by Wen et al. (2010) [6] and Yang et al. (2015) [50] The generalized parameters for soil moisture calculation and saturated hydraulic conductivity of different soil textures are shown in Table 2.

In addition, the aggregation index Ω of different land cover types is also an important parameter which is related to the calculation of vegetation (see Equations (12) and (13)). The values of Ω of different land types are listed in Table 3.

Table 3. The values of Ω of different land cover types.

Land Cover Types	Ω	Land Cover Types	Ω
Evergreen coniferous forest	0.6	Permanent wetlands	0.9
Evergreen broad-leaf forest	0.8	Farmland	0.9
Deciduous coniferous forest	0.6	Urban and construction land	0.9
Deciduous broad-leaf forest	0.8	Crops and natural vegetation ecotone	0.9
Mixed forest	0.7	Snow/ice	-
Closed shrublands	0.8	Bare and sparse vegetation	-
Open shrublands	0.8	Water area	-
Grassland	0.9		

4. Results and Analyses

4.1. Simulation of the Current Situation of Blue Water and Green Water

In order to analyze the change of blue water and green water, based on the water balance principle and the SPAC principle, each component value of blue water and green water in the initial year (2003) and the current year (2013) was simulated using the SVAT model to calculate the evapotranspiration of vegetation in leaky regions in the environs of Guiyang (Table 4).

Table 4. Component values of blue water and green water in 2003 and 2013.

Year	*Vc*	*Pr*	*Eps*	*E-plant*	*Inter*	*Soil-w*	*Runoff*	*Leakage*	*Green-w*
2003	49.75	968.23	91.67	182.86	35.05	151.77	506.87	83.31	461.36
2013	60.93	922.06	82.67	204.23	40.04	131.73	463.38	70.24	458.68

Notes: *Vc* is vegetation coverage (unit: %), *Pr* is precipitation (unit: mm), *Eps* is soil evaporation (unit: mm), *E-plant* is vegetation transpiration (unit: mm), *Inter* is vegetation interception (unit: mm), the unit of *Runoff* is mm, Soil-w is soil water storage (unit: mm), the unit of *Leakage* is mm, and *Green-w* is green water (unit: mm).

In addition, it is found through "Guiyang Statistical Yearbook" issued by Guiyang Municipal Statistics Bureau [77] that the climatic data of the two chosen years have a high similarity (Table 5). According to the SPAC principle, if the climate of the two years had little change, the effects which come from changed vegetation and changed soil on evapotranspiration can be compared.

Table 5. The main climate indexes of 2003 and 2013.

Year	*At* (°)	*Rh* (%)	*Sh* (h)	*Pr* (mm)	*Rain* (Day)	*Frost* (Day)	*Fog* (Day)	*Dew* (Day)	*Snow* (Day)	*Freeze* (Day)
2003	14.9	80.0	915	933.7	95	9	25	121	7	15
2013	15.1	79.0	1230.7	937.2	211	9	31	124	13	15

Notes: *At* is average temperature, *Rh* is relative humidity, *Sh* is sunshine hours, *Pr* is precipitation, *Rain* is rainy days, *Frost* is frost days, *Fog* is fog days, *Dew* is dew days, *Snow* is snow days, and *Freeze* is frozen days. The contents in brackets are units.

Table 4 shows that blue water (*Runoff*) is 506.87 and 463.38 mm/km^2 and that green water (*Eps*, *E-plant*, *Inter,* and *Soil-w*) is 461.36 and 458.68 mm/km^2 in 2003 and 2013, respectively. Green water accounts for <50% of precipitation in both years, which is far below the global average (65%). Furthermore, leakage volume in 2003 and 2013 amounts to 8.60% and 7.62%, respectively, which indicates the scale of the adjustment required.

The spatial distribution of leakage shows that the spatial distribution of leakage has no obvious correlation with vegetation coverage (Figure 4d). Figure 5 shows that the severe leaky areas where the leakage volume is >180 mm, are all located in areas of loam; thus, the essential cause of leakage should be related to soil properties. In fact, the influence of the special geological structure of limestone should also be considered when leakage in karst regions is analyzed. Because the rock properties have not been incorporated in the SVAT model, in this article, instead of the cause of leakage, the measure of

leakage reduction was analyzed in degraded karst area where the ecological environment suffered severe damage.

As seen from Figure 4a,b, the average leakage volume in 2003 is somewhat higher than that in 2013, although the spatial distribution of leakage is consistent between the years. The entire leaky area is about 3805 km^2, which accounts for 50.77% of the study area. The area of severe leakage is 885 km^2 in 2013, which accounts for 23.26% of the leaky area.

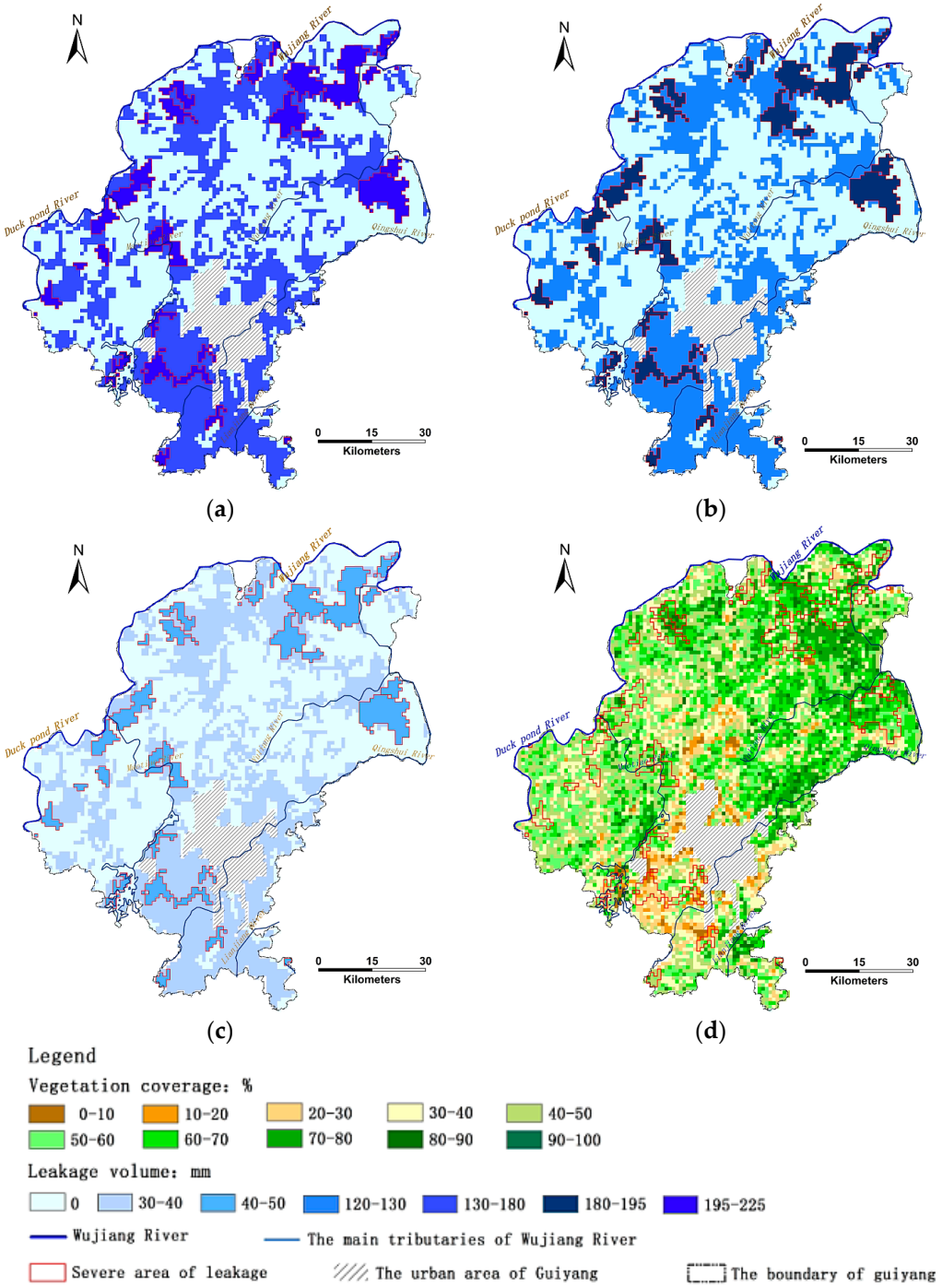

Figure 4. Spatial distribution of leakage volume in the environs of Guiyang: (**a**) in 2003; (**b**) in 2013; (**c**) as soil is thickened by 20 cm based on 2013; and (**d**) spatial distribution of severe leaky area and vegetation coverage in 2013. Note: The red boundary defines areas of severe leakage (>180 mm).

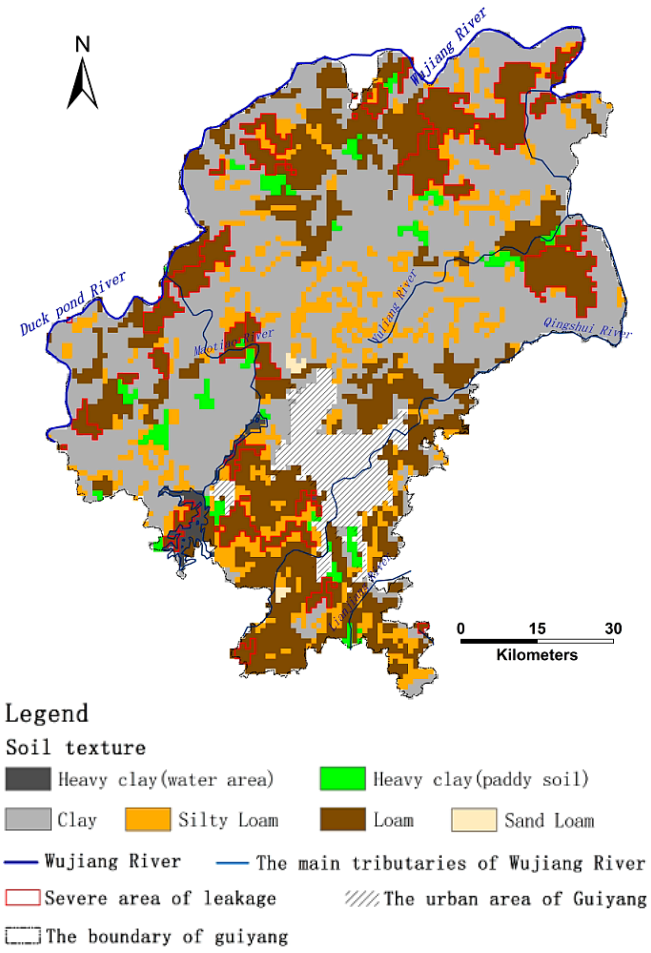

Figure 5. The distribution of soil texture in the environs of Guiyang.

4.2. Validation of the Model Calculation Results

Because of the lack of observational data on leakage, a method of indirect validation was adopted to assess the precision of the modeling. According to the principle of the water balance, the assessment of the accuracy of leakage can be achieved by validating each hydrological index incorporated in the calculation process.

First, the verification value of vegetation interception was derived from field observation data obtained in Kaiyang County in Guiyang by Zhang et al. (2007) [78]. The verification values of soil evaporation, plant transpiration, and saturated water content were obtained from calculation results for Puding County near Guiyang, these data were verified by Zhang et al. (2009) [79]. The verification value of soil water storage was converted according to the ratio of soil water storage calculated by Wen et al. (2010) [6] in Guiyang and surrounding areas. The verification value of runoff was obtained from the "Guiyang Water Resources Bulletin" issued by the Water Administration Department of Guiyang [80]. The simulation values and verification values are shown in Table 6.

Table 6. Simulation and verification values. Unit: mm.

Data Source	*Eps*	*E-plant*	*Inter*	*Soil-w*	*Satur-w*	*Runoff*
Simulation values (2003)	91.67	182.86	35.05	151.77	68.46	506.87
Simulation values (2013)	82.67	204.23	40.04	131.73	61.49	463.38
Verification values	85.28	197.52	48.65	170.57	96.74	417.90

Notes: *Satur-w* is soil saturated water content (unit: mm), other units were given above.

Table 6 shows that although the differences in soil water storage and saturated water content between the simulation and verification values are some larger, the differences in other values are relatively smaller. The simulation value of soil water storage is much larger than that of verification value because the verification value is calculated with reference to the soil moisture content after six days without rain, which is obviously lower than normal values. The soil saturated water content of verification value is larger than that of simulation value, which is mainly because the verification value was obtained from a small watershed while the study area is much larger. In addition, Figure 6 shows that the distribution of simulation values was close to the 45° line, which indicates a good similarity between the verification values and the calculation results of each hydrological variable computed by the SVAT model. Therefore, the value of *leakage*, which is associated with other calculation results such as *Eps*, *E-plant*, *Soil-w*, etc., according to the principle of SPAC and water balance theory, should have good credibility.

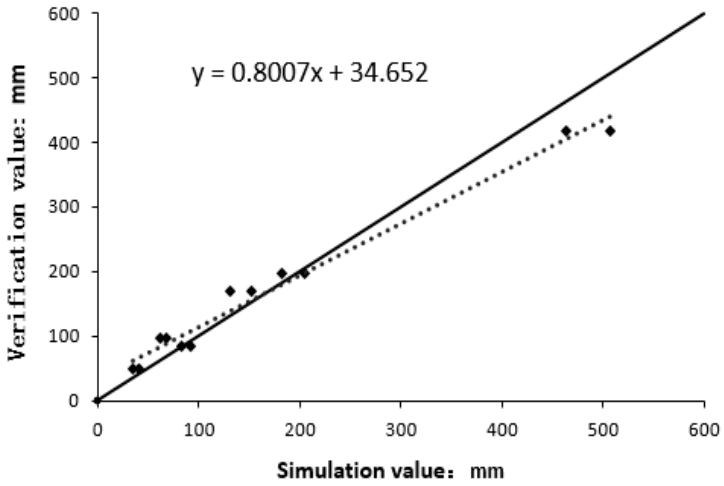

Figure 6. Degree of similarity between the simulation value and verification value.

Second, in 2013, the simulation of leakage volume of each administrative district of Guiyang (Figure 7) has the same change trend as the quantity of groundwater issued by the Water Administration Department (Table 7 and Figure 8), which shows the simulation results have good credibility. The groundwater volumes of the administrative districts in 2003 were issued based on old administrative districts and boundaries; therefore, they are not suitable for comparison of the spatial distribution of groundwater with that of leakage in 2003.

Table 7. Groundwater and simulated values of leakage in each district of Guiyang. Unit: million m^3.

Value in 2013	Municipal District	Kaiyang	Xifeng	Xiuwen	Qingzhen
Groundwater	367.50	318.10	169.70	159.80	181.80
Leakage	168.84	136.03	79.70	57.96	83.33

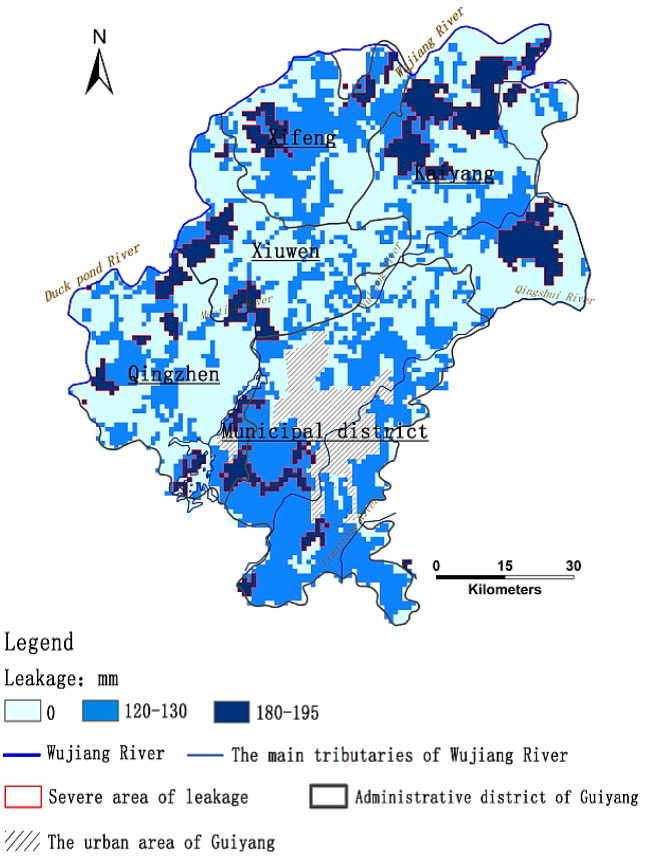

Figure 7. The distribution of leakage in each administrative district of Guiyang in 2013.

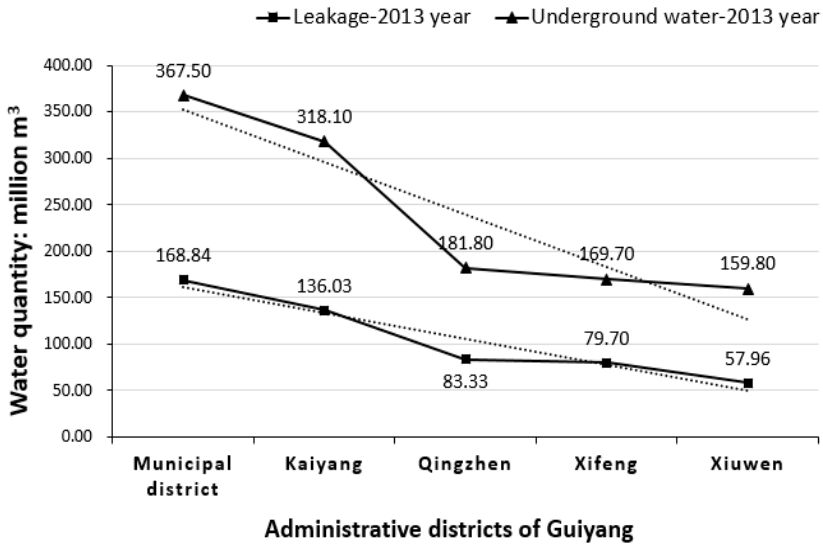

Figure 8. Contrast between simulation of leakage and groundwater in each district of Guiyang.

4.3. Impact of Vegetation Increase on the Reduction of Leakage Volume

Given precipitation and vegetation coverage changed simultaneously from 2003 to 2013 (Table 4), in order to ascertain whether precipitation or vegetation coverage was the primary cause of leakage reduction, it is necessary to analyze the leakage change tendency under the condition that vegetation coverage changes while precipitation does not. The simulation results are shown in Table 8.

Table 8. Impact of vegetation coverage increase on leakage.

Scenario	*Vc*	*Pr*	*Eps*	*E-plant*	*Inter*	*Soil-w*	*Runoff*	*Leakage*	*Green-w*
2003 Year	49.75	968.23	91.67	182.86	35.05	151.7730	506.87	83.3116	416.09
2007 Year	55.93	968.23	87.56	204.08	37.83	149.8836	488.87	82.3238	439.80
2013 Year	60.93	968.23	82.23	224.57	42.97	149.8378	468.62	82.2953	463.91
VC + 1%	61.91	968.23	81.57	228.64	43.70	149.8375	464.48	82.2950	468.79
VC + 2%	62.91	968.23	80.76	232.87	44.46	149.8366	460.29	82.2945	473.74
VC + 5%	65.93	968.23	78.24	246.11	46.89	149.8354	447.16	82.2934	489.20
VC + 10%	70.93	968.23	73.61	269.80	51.40	149.8320	423.58	82.2919	516.59

A series of change trends can be found from Table 8 and Figure 9.

(1) When precipitation is unchanged, the increase of vegetation coverage leads to a trend of decrease of leakage.

(2) With the increase of vegetation coverage, the values of *Eps*, *E-plant*, and *Inter* all increase synchronously and runoff reduces accordingly, while soil water storage and leakage only appear to show slight reductions. The simulation results implied that the greatest contributions of an increase in vegetation are the increase in water consumed by the plant and the reduction of runoff, which benefit the transformation of blue water into green water.

(3) Figure 9a shows there is a positive correlation between vegetation growth and the increase of green water, which means that vegetation growth plays an important role in converting blue water into green water. According to the SPAC principle, leakage is mainly related to soil water storage and, thus, increasing vegetation could not significantly decrease leakage.

(4) The simulation results shows that when vegetation coverage increases from 50% to 56%, the amount of leakage reduction is about 1 mm/km^2 and the extent of the reduction is the largest (1.19%).

(5) Figure 9b (note, the unit of leakage volume is converted to million m^3 for convenience of comparison) shows that, once vegetation coverage ratio is >56%, the trend of leakage reduction slows sharply with further increase of vegetation coverage (i.e., an increase in vegetation coverage of 1%, has an average contribution of <1/1000 to leakage reduction). Although the nonlinearity may be due to model sensitivity and could be model depended, given vegetation coverage is not the crucial factor on leakage in karst regions, the simulative relationship between vegetation and leakage may have a certain reference significance.

(6) As far as the analysis of simulation results, there might be a threshold value of vegetation coverage increase. As the vegetation coverage in study area in 2013 had exceeded this value (56%), a simulation of other means for reducing leakage quantity is necessary.

(7) The presence of a threshold value means that although the variation of vegetation coverage can affect the quantity of leakage in degraded karst areas, its role is limited and it is not the only factor.

Because the average ratio of vegetation coverage had already exceeded 60% by 2013, it is necessary to explore a better method for reducing leakage in regions where the vegetation coverage ratio is >50%. According to the principle of SPAC, in addition to vegetation and precipitation, the thickness of the soil is another major influential factor on leakage.

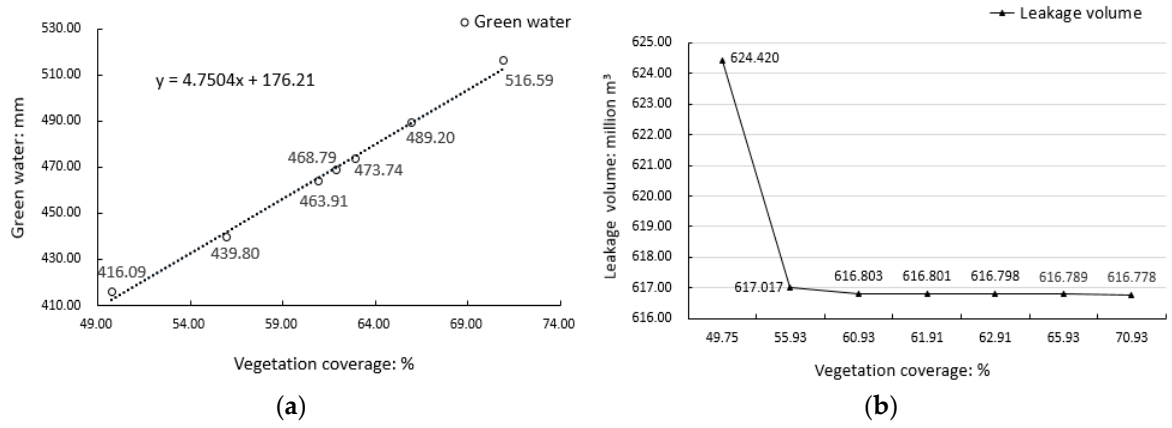

Figure 9. (**a**) Linear dependence relation between vegetation coverage and green water; and (**b**) telationship between vegetation coverage increase and leakage reduction.

4.4. Impact of Increasing Soil Thickness on the Reduction of Leakage

It was assumed that precipitation and vegetation coverage were unchanged. Therefore, by selecting the values of different soil thickness based on the principle of facilitating the SVAT model calculation and analysis, the impact of soil thickness on blue water and green water transformation was revealed by simulations in which the soil thickness was increased by 10 and 20 cm based on 2013 data. The simulation results are shown in Table 9.

Table 9. Main indices of blue water and green water variation with different soil thickness (unit: mm).

Parameter	2013	Soil Thickness Thickened by 10 cm	Difference Value after Soil Thickness Increased by 10 cm	Soil Thickness Thickened by 20 cm	Difference Value after Soil Thickness Increased by 20 cm
Eps	81.79	89.20	7.41	96.50	14.71
E-plant	206.80	206.80	0	206.80	0
Inter	42.97	42.97	0	42.97	0
Soil-w	149.81	195.62	45.81	249.92	100.11
Runoff	486.87	433.64	−53.22	372.05	−114.82
Leakage	82.29	36.48	−45.81	17.82	−64.47
Green-w	499.36	552.59	53.23	614.18	114.82

From Table 9, a number of change features can be determined by comparison of the simulation results.

(1) Increasing the soil thickness by 10 cm leads to a reduction of leakage of 55.67% (i.e., 45.81/82.29), and the decreased quantity (45.81 mm) is right equaled to the increased quantity of soil water storage. Increasing the soil thickness by 20 cm leads to a reduction of leakage of 78.35 (i.e., 64.47/82.29), and the decreased quantity of leakage (64.47 mm) is less than the increased quantity of soil water storage (100.11 mm) (Figure 4c). This means that with the increase of soil thickness, more and more precipitation is retained in the soil in the form of green water, resulting in a substantial reduction of leakage, which shows increasing soil thickness has a good effect on reducing leakage.

(2) All the reduction in the volume of leakage caused by increasing soil thickness is transformed into green water. Increasing the soil thickness by 10 cm leads to the transformation of 53.22 mm of runoff into green water, which is equivalent to 10.93% (i.e., 53.22/486.87) of the runoff in 2013. Increasing the soil thickness by 20 cm leads to the transformation of 114.82 mm of runoff into green water, which is equivalent to 23.58% (i.e., 114.82/486.87) of the runoff in 2013. Thus, the effect of soil thickness on the transformation of green water is very apparent.

(3) When soil thickness is thickened by 10 cm, based on 2013 data, leakage decreases by 36.48 mm, a decrease of 55.67% (i.e., 45.81/82.29). If the thickness of the soil is increased by a further 10 cm, the leakage decreases by a further 18.66 mm, i.e., a decrease of 22.67% (i.e., 18.66/82.29). This shows that the greatest reduction of leakage occurs when the soil thickness is increased by 10 cm; further increases in soil thickness have a gradually weakening effect.

(4) When the soil thickness is thickened by 20 cm, based on 2013 data, surface runoff is reduced considerably by about 50.35 mm. According to research by Tennant (1976) [81], aquatic ecosystems would not experience adverse effects unless the reduction in runoff was >40%; however, given that the projected decrease is 23.58% under the scenario of soil thickened by 20 cm, further increases in soil thickness might have a negative influence on aquatic ecosystems. Furthermore, under this scenario, the proportion of green water is 61.57% of precipitation, which is close to the world average of 65%; therefore, further increasing of the soil thickness could be considered unnecessary.

(5) When the soil thickness is thickened by 20 cm, based on 2013 data, *Runoff* decreases by 860 million m^3 (114.82 mm/km^2), *Soil-w* increases by 750 million m^3 (100.10 mm/km^2), *Leakage* decreases by 483 million m^3 (64.47 mm/km^2), and *Eps* increases by 110 million m^3 (14.71 mm/km^2); however, the volumes of *E-plant* and Inter of vegetation remain unchanged. The increase in the volumes of *Eps* and *Soil-w* equal that of the precipitation decrease, i.e., (1.10 + 7.50 = 36.49 − 27.89) 860 million m^3, which means the overall water volume is balanced and that the results of the simulation are reasonable.

5. Discussion

By means of the SVAT model, the distribution of blue water and green water in the environs of Guiyang was simulated. Furthermore, through calculation and analysis, two methods with which the hard-to-use leaked blue water could be transformed into green water for ecologic consumption were proposed. However, from the perspective of application, the specific spatial location and scope, as well as the specific transformational measures still need further in-depth analysis and discussion.

5.1. Analysis of the Regional Distribution of Increasing Vegetation Measures

According to the SPAC principle, changing regional vegetation coverage is an important measure for adjusting the proportion of blue water and green water. Furthermore, previous calculation results have shown that when vegetation coverage increases from 50% to 56%, the reduction of leakage volume is about 1 mm/km^2 and the extent of the reduction is much greater than that after vegetation coverage exceeds 56%. Therefore, it is necessary to identify the leaky forest and grassland based on land use type (Figure 10a) where vegetation coverage is <50% as areas for adjustment (Figure 10b) by increasing vegetation.

As shown in Figure 10a,b, the leaky area where vegetation coverage is <50% and land use is forest and grass is 1248 km^2, which accounts for 50.88% of the leaky forest and grassland, and for 32.80% of the entire leaky area (3805 km^2).

Thus, several ideas for increasing vegetation could be taken into account based on a comparison of the distribution of vegetation coverage in 2003 and 2013 (Figure 10c,d) and leakage in 2013 (Figure 10b).

(1) The region identified as typical leaky area where leakage is >180 mm and vegetation coverage <50% has an area of 393 km^2 (Figure 10c,d), which was about 44.1% of the severe leaky area (885 km^2) where leakage is >180 mm. The typical leaky area would be high priority for reducing leakage by increasing vegetation.

(2) On average, vegetation coverage increased by about 10% in the environs of Guiyang from 2003 to 2013. The regions in areas of typical leakage, where vegetation coverage did not change obviously (131 km^2) or became degraded (36 km^2) occupy about 167 km^2 in total, which accounted for 41.64% of the typical leaky region and were important regarding vegetation restoration (Figure 11).

(3) The reason for the lack of vegetation growth during 2003–2013 in areas where the vegetation coverage decreased or remained unchanged could be attributable to anthropogenic activity or the terrain. Therefore, it would be necessary to adopt appropriate measures according to the actual situation when adjustments were considered. If it was anthropogenic activity that caused the lack of growth in vegetation coverage, measures of increasing vegetation should be taken.

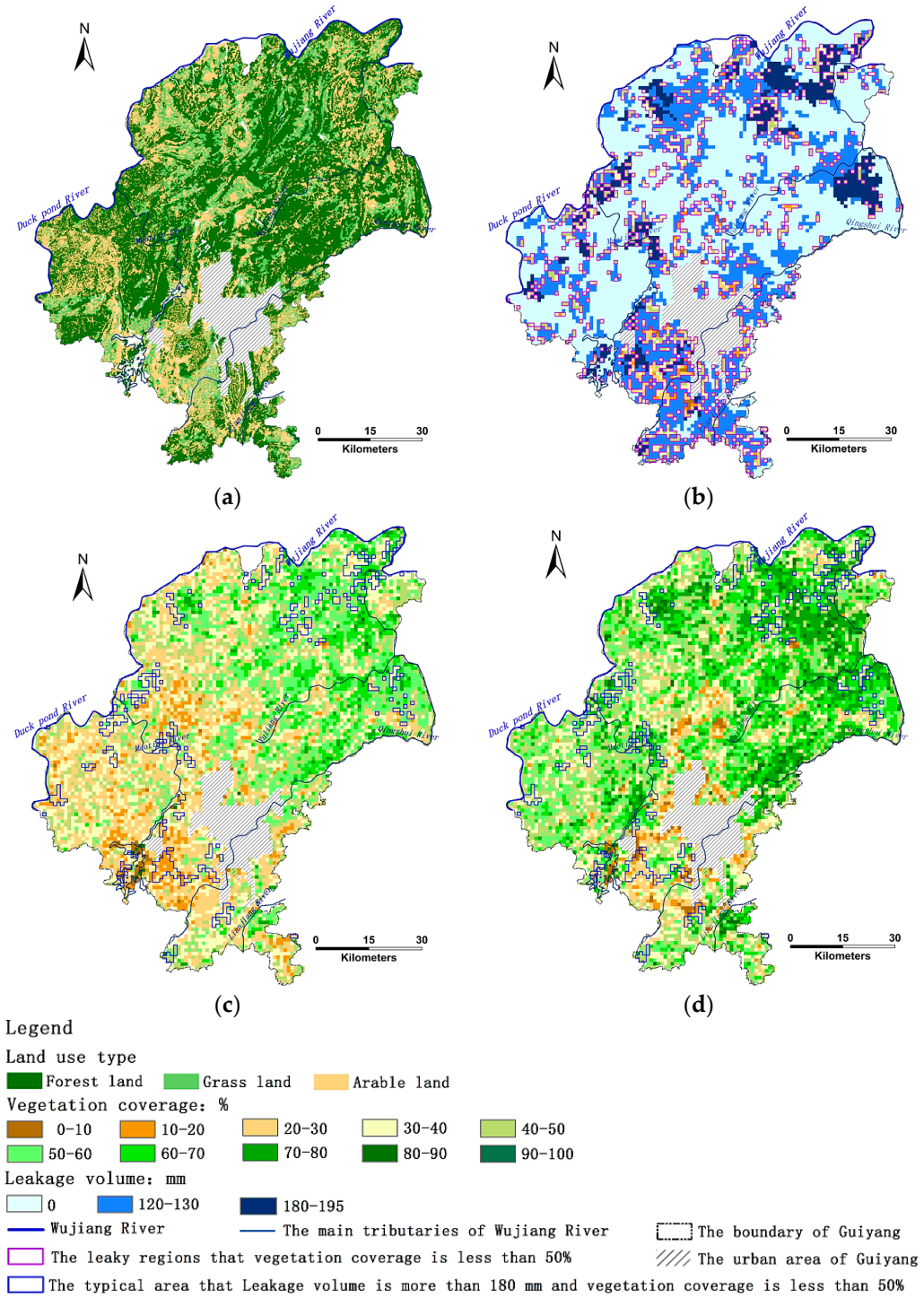

Figure 10. (**a**) The type of land use; (**b**) leaky regions where vegetation coverage is <50% and land use cover is forest and grassland in 2013; and (**c**) vegetation coverage in 2003; and (**d**) in 2013.

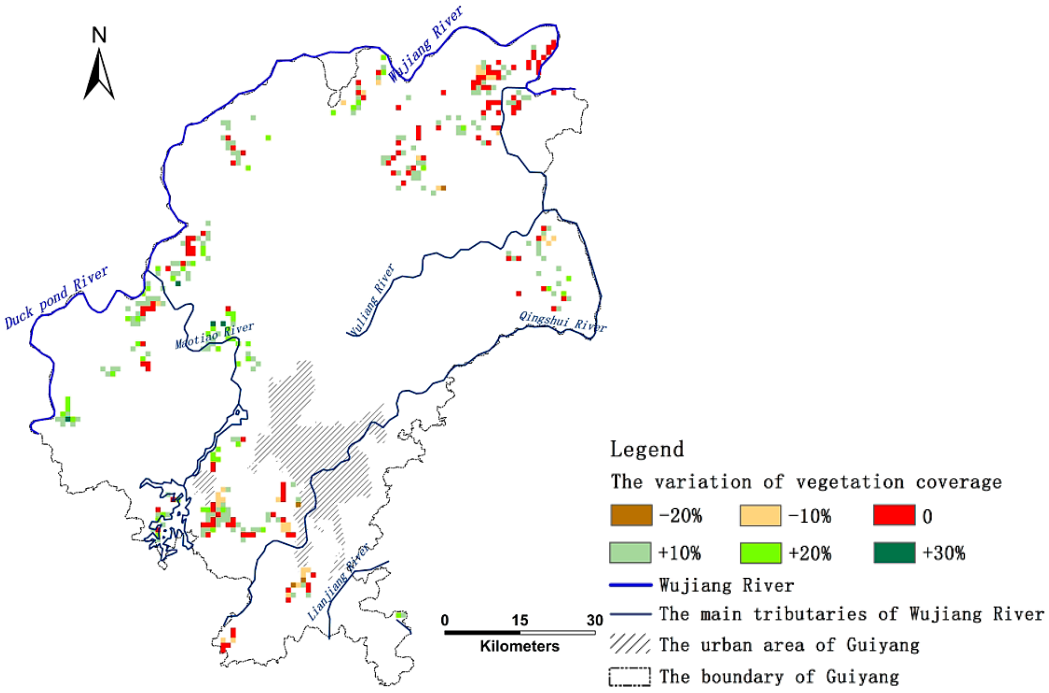

Figure 11. Variation of vegetation coverage from 2003 to 2013 in typical leaky area.

5.2. Analysis of the Regional Distribution of Increasing the Thickness of Soil

Theoretically, if adjustment measures were not restricted by natural conditions and economic costs, all leakages of blue water could be reduced by increasing soil thickness in leaky regions. However, the reality is often restricted by economic and natural factors. Therefore, some special areas where increasing soil is necessary should be proposed, and the corresponding measures should also be paid attention to. Based on the previous simulation results and investigation, here are some concerns:

(1) The regions where leakage could be decreased by increasing the vegetation coverage that have been extracted in the previous section. Therefore, some areas with severe leakage, where vegetation coverage is >50% (Figure 12), could be classified as regions urgently in need of adjustment of soil thickness; these regions occupy an area of about 492 km^2.

(2) There were some areas where vegetation coverage was >50% and leakage was >180 mm, which implies that enhancing vegetation coverage was just one method for reducing leakage. Meanwhile, the essential cause of a large amount of leakage in karst regions might be related to the soil texture (Figure 5) and the characteristics of the bedrock.

(3) If the lack of growth of vegetation coverage in forest and grassland regions in areas of severe leakage, mentioned in Section 5.1, was not due to anthropogenic activity or steep terrain, it should be adjusted by increasing the thickness of soil.

(4) Led by the local water administrative department, the "Terracing of cultivated sloping land" project was conducted in some degraded karst areas, which has added many levels of terraces through increasing soil thickness and flattening soil on the slopes (Figure 13a,b). This practice showed that the project was very beneficial to the conservation of soil and water in degraded karst areas [82,83]. Luo et al. (2007) [84] found that the annual rates of water conservation, soil conservation, and increase of the maize yield reached 37.4%, 71.2%, and 36.4%, respectively, on the terraced slopes in a degraded karst area. Thus, not only were the losses of soil and water effectively reduced, but rural economic income was also improved. Therefore, increasing soil thickness could be proposed as an important specific measure to reduce leakage and to transform blue water into green water.

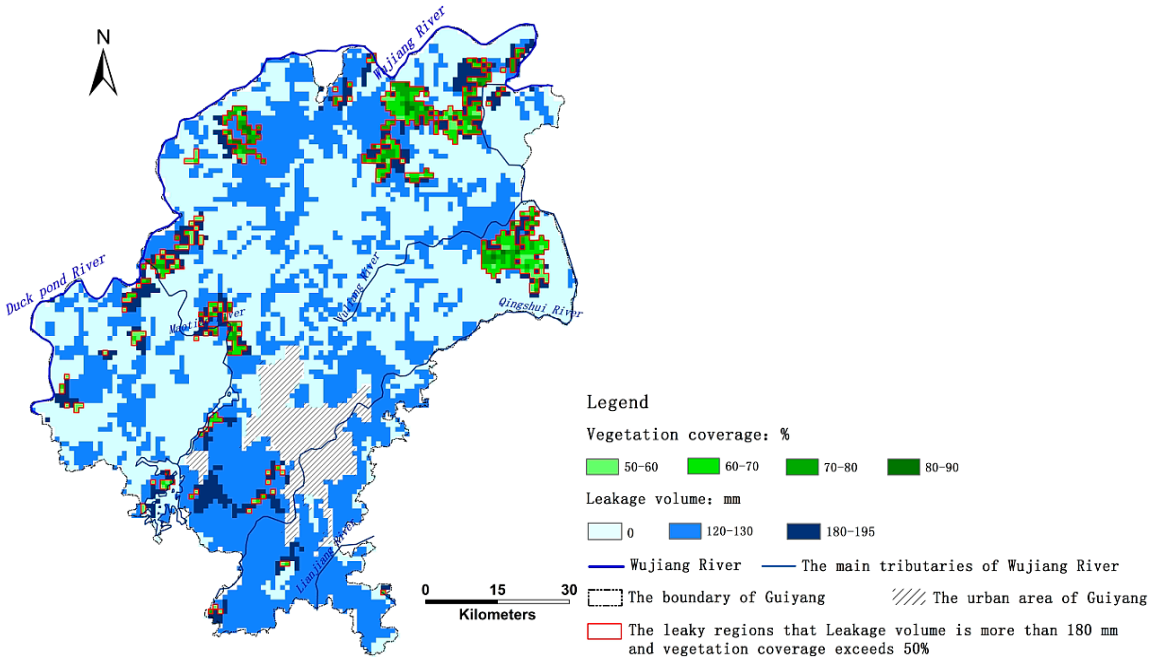

Figure 12. Leaky regions where the leakage volume is >180 mm and vegetation coverage is >50%.

(**a**) (**b**)

Figure 13. (**a**,**b**) Scenes of the "Terracing of cultivated sloping land" project in Kaiyang County, Guiyang.

5.3. Detailed Analysis of Effect of Adjusting Soil Thickness

According to the simulation results in Section 4.3, once the vegetation coverage reaches a certain proportion, its effect on reducing leakage becomes increasingly limited. However, at the same time, leakage can be decreased considerably by increasing the thickness of the soil (see Section 4.4). To further explore the contribution of increased soil thickness to reduced leakage, it is necessary to analyze the contribution made to leakage reduction by a soil layer thickened by 20 cm under different precipitation scenarios, i.e., a rainy year, normal year, and dry year. The simulation results are shown in Table 10.

Table 10. Impact of increasing soil thickness on leakage reduction under different precipitation scenarios.

Parameter	2013 (Rainy)	2013 (Rainy) Soil Thickness Thickened by 20 cm	2013 (Normal)	2013 (Normal) Soil Thickness Thickened by 20 cm	2013 (Dry)	2013 (Dry) Soil Thickness Thickened by 20 cm
Pr	1336.16	1336.16	1094.10	1094.10	774.58	774.58
Eps	88.94	107.01	82.30	99.08	73.93	85.89
E-plant	198.27	198.27	198.28	198.28	198.29	198.29
Inter	53.57	53.57	46.80	46.80	36.55	36.55
Soil-w	151.43	257.43	150.49	252.60	148.63	244.80
Runoff	843.94	719.87	615.32	497.33	317.18	208.96
Leakage	82.94	23.06	82.58	19.53	81.80	14.45

Table 10 provides the following findings:

(1) In the rainy year scenario, increasing the soil thickness by 20 cm, based on 2013 data, decreases leakage by 72.19% (59.88 mm).

(2) In the normal year scenario, increasing the soil thickness by 20 cm, based on 2013 data, decreases leakage by 76.35% (63.05 mm).

(3) In the dry year scenario, increasing the soil thickness by 20 cm, based on 2013 data, decreases leakage by 82.34% (67.35 mm).

(4) In the dry year scenario, by increasing the soil thickness by 20 cm, based on 2013 data, the decrease of leakage is greater than in the normal and dry year scenarios. The sequence of leakage reduction in descending order is dry year scenario > normal year scenario > rainy year scenario, which effectively relieves the ecological water shortage of vegetation.

It reveals that by increasing the soil thickness, additional quantities of leaked blue water will be transformed into green water, effectively raising the amount of ecological water use. The effect of thickened soil on leakage and the range of reduction under the different precipitation scenarios are shown in Figure 14.

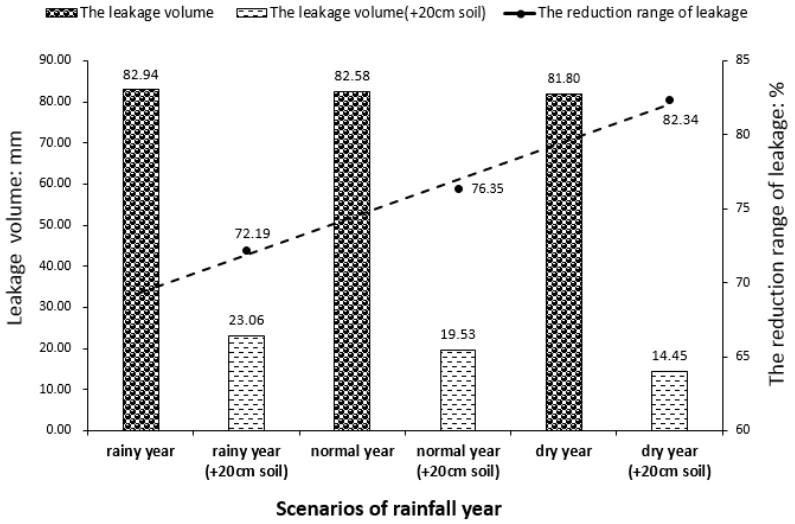

Figure 14. Reduction of leakage under different precipitation scenarios and the range of reduction.

6. Conclusions

According to the SPAC principle, by using the SVAT model combined with the geographical analysis approach, the distribution of blue water and green water in the environs of Guiyang (China), a typical degraded karst area, was simulated for 2003 and 2013. The effects of changes in precipitation,

vegetation coverage, and soil thickness on the leakage of blue water were calculated and visually presented, the principal findings were as follows.

(1) In 2013, the precipitation volume in the environs of Guiyang was 922 mm, of which blue water and green water amounted to 463.38 mm (50.25%) and 458.68 mm (49.75%), respectively. The proportion of green water was far below the global average (65%). Furthermore, the leakage volume (70 mm) accounted for 15.16% of blue water and 7.62% of precipitation, which indicates the scope of the potential adjustment.

(2) Our model simulation shows that vegetation growth played an important role in converting blue water into green water; however, once it increased to 56%, its contribution to reducing leakage (blue water) decreased sharply, which indicated other adjustment measures such as increasing soil thickness should be conducted.

(3) In typical leaky regions where leakage is >180 mm and vegetation coverage is <50%, areas where vegetation coverage had not changed obviously from 2003 to 2013 accounted for 31.3% of the typical leaky regions. Furthermore, negative vegetation growth was found out in a few areas, indicating the urgent need to increase vegetation coverage in these leaky areas.

(4) When soil thickness was increased by 20 cm, based on 2013 data, leakage decreased by 78.35% (483.20 million m^3), and all the unavailable leaked blue water was transformed into green water. Furthermore, the sequence of leakage reduction under different precipitation scenarios in descending order was dry year > normal year > rainy year, which significantly improves the utilization ratio of water resources and raises the amount of plant ecological water use. The practice showed the "Terracing of cultivated sloping land" project (i.e., increasing soil thickness) was an effective conversion measure of blue water into green water in degraded karst areas.

(5) Despite the inevitable idealized simulation process determined by the parameterizations and model sensitivity, the method of SVAT model combined with geographical distribution analysis and the transformation from blue water into green water, which avoids constructions of hydraulic engineering, could provide a new technical solution to improve the utilization of water resources in degraded karst areas. Thus, it has important significance for overcoming similar problems.

Acknowledgments: We acknowledge all reviewers and editors for their valuable advice. This research was supported by the National Natural Science Foundation of China (Grant No. 41271414), the project of National Natural Science Foundation of China: "Security paradigm of water resource utilization and hydrology variability in ungauged watershed of Albea Lake", the Special Fund of Beijing Key Laboratory Jointly Building Project, and the Fundamental Research Funds for the Central Universities.

Author Contributions: Ke Chen played an important role in the conception of the study, performing the model calculation, data analyses and drafting and revising the manuscript. Shengtian Yang and Zongli Li played an important role in the conceptual framework of this paper. Changsen Zhao contributed to the research progress, domestic and overseas. Ya Luo and Qiuwen Zhou contributed to the data validation. Zhiwei Wang contributed to graph facture. Xiaolin Liu and Juan Bai assisted in the SVAT model calculation. Yabing Guan and Xinyi Yu contributed to data gathering and processing. All authors read and approved the final manuscript.

Conflicts of Interest: The authors declare no conflict of interest.

References

1. Falkenmark, M. Coping with water scarcity under rapid population growth. In Proceedings of the Conference of SADC Ministers, Pretoria, South Africa, 23–24 November 1995; pp. 23–24.
2. Lathuillière, M.J.; Coe, M.T.; Johnson, M.S. A review of green- and blue-water resources and their trade-offs for future agricultural production in the Amazon Basin: What could irrigated agriculture mean for Amazonia? *Hydrogeol. Earth Syst. Sci.* **2016**, *20*, 2179–2194. [CrossRef]
3. Ringersma, J.; Batjes, N.; Dent, D. *Green Water: Definitions and Data for Assessment*; ISRIC, World Soil Information: Wageningen, The Netherlands, 2003.
4. Stewart, B.A.; Peterson, G.A. Managing green water in dryland agriculture. *Agron. J.* **2015**, *107*, 1544–1553. [CrossRef]

5. Falkenmark, M.; Rockstrom, J. The new blue and green water paradigm: Breaking new ground for water resources planning and management. *J. Water Resour. Plan. Manag. ASCE* **2006**, *132*, 129–132. [CrossRef]
6. Wen, Z.; Yang, S.; Song, W.; Bai, X.; Gao, F.; Liu, W. The numerical simulation on green water cycle of typical vegetation types in karst area. *Geogr. Res.* **2010**, *29*, 1841–1852. (In Chinese)
7. Hoekstra, A.Y.; Chapagain, A.K.; Aldaya, M.M.; Mekonnen, M.M. *The Water Footprint Assessment Manual: Setting the Global Standard*; Earthscan: London, UK; Washington, DC, USA, 2011; p. 203.
8. Launiainen, S.; Futter, M.N.; Ellison, D.; Clarke, N.; Finer, L.; Hogbom, L.; Lauren, A.; Ring, E. Is the water footprint an appropriate tool for forestry and forest products: The fennoscandian case. *Ambio* **2014**, *43*, 244–256. [CrossRef] [PubMed]
9. Quinteiro, P.; Dias, A.C.; Silva, M.; Ridoutt, B.G.; Arroja, L. A contribution to the environmental impact assessment of green water flows. *J. Clean. Prod.* **2015**, *93*, 318–329. [CrossRef]
10. Zang, C.F.; Liu, J.; van der Velde, M.; Kraxner, F. Assessment of spatial and temporal patterns of green and blue water flows under natural conditions in inland river basins in northwest China. *Hydrol. Earth Syst. Sci.* **2012**, *16*, 2859–2870. [CrossRef]
11. Liu, J.; Zehnder, A.J.B.; Yang, H. Global consumptive water use for crop production: The importance of green water and virtual water. *Water Resour. Res.* **2009**, 45. [CrossRef]
12. Ballesteros, D.; Malard, A.; Jeannin, P.Y.; Jimenez-Sanchez, M.; Garcia-Sansegundo, J.; Melendez-Asensio, M.; Sendra, G. Karsys hydrogeological 3d modeling of alpine karst aquifers developed in geologically complex areas: Picos de Europa National Park (Spain). *Environ. Earth Sci.* **2015**, *74*, 7699–7714. [CrossRef]
13. Wei, X.P.; Yan, Y.; Xie, D.T.; Ni, J.P.; Loaiciga, H.A. The soil leakage ratio in the mudu watershed, China. *Environ. Earth Sci.* **2016**, *75*. [CrossRef]
14. Qin, L.Y.; Bai, X.Y.; Wang, S.J.; Zhou, D.Q.; Li, Y.; Peng, T.; Tian, Y.C.; Luo, G.J. Major problems and solutions on surface water resource utilisation in karst mountainous areas. *Agric. Water Manag.* **2015**, *159*, 55–65. [CrossRef]
15. Jourde, H.; Lafare, A.; Mazzilli, N.; Belaud, G.; Neppel, L.; Dorfliger, N.; Cernesson, F. Flash flood mitigation as a positive consequence of anthropogenic forcing on the groundwater resource in a karst catchment. *Environ. Earth Sci.* **2014**, *71*, 573–583. [CrossRef]
16. Guo, F.; Jiang, G.H.; Yuan, D.X.; Polk, J.S. Evolution of major environmental geological problems in karst areas of southwestern China. *Environ. Earth Sci.* **2013**, *69*, 2427–2435. [CrossRef]
17. Green, R.T.; Painter, S.L.; Sun, A.; Worthington, S.R. Groundwater contamination in karst terranes. *Water Air Soil Pollut. Focus* **2006**, *6*, 157–170. [CrossRef]
18. Breitenbach, S. Karst hydrogeology and geomorphology. *Erde* **2008**, *139*, 121–122.
19. Wei, Y.; Yu, L.F.; Zhang, J.C.; Yu, Y.C.; Deangelis, D.L. Relationship between vegetation restoration and soil microbial characteristics in degraded karst regions: A case study. *Pedosphere* **2011**, *21*, 132–138. [CrossRef]
20. Huang, Q.H.; Cai, Y.L. Mapping karst rock in southwest China. *Mt. Res. Dev.* **2009**, *29*, 14–20. [CrossRef]
21. Deng, Y.; Jiang, Z.C. Characteristic of rocky desertification and comprehensive improving model in karst peak-cluster depression in Guohua, Guangxi, China. *Procedia Environ. Sci.* **2011**, *10*, 2449–2452. [CrossRef]
22. Wan, L.; Zhou, J.X.; Guo, H.Y.; Cui, M.; Liu, Y.G. Trend of water resource amount, drought frequency, and agricultural exposure to water stresses in the karst regions of South China. *Nat. Hazards* **2016**, *80*, 23–42. [CrossRef]
23. Gams, I.; Gabrovec, M. Land use and human impact in the Dinaric karst. *Int. J. Speleol.* **1999**, *28*, 55–70. [CrossRef]
24. Yassoglou, N.J.E.G.; D'Angelo, M.; Zanolla, C. History of desertification in the european mediterranean. In *Indicators for Assessing Desertification in the Mediterranean, Proceedings of the International Seminar Held in Porto Torres, Italy, 18–20 September 1998*; Enne, G., D'Angelo, M., Zanolla, C., Eds.; Nucleo Ricerca Desertificazion, University of Sassari: Athens, Greece, 2000.
25. Tong, X.; Wang, K.; Yue, Y.; Brandt, M.; Liu, B.; Zhang, C.; Liao, C.; Fensholt, R. Quantifying the effectiveness of ecological restoration projects onlong-term vegetation dynamics in the karst regions of southwest China. *Int. J. Appl. Earth Obs. Geoinf.* **2016**, *54*, 105–133. [CrossRef]
26. Jiang, Z.; Lian, Y.; Qin, X. Rocky desertification in southwest China: Impacts, causes, and restoration. *Earth Sci. Rev.* **2014**, *132*, 1–12. [CrossRef]
27. Wang, S.J.; Liu, Q.M.; Zhang, D.F. Karst rocky desertification in southwestern China: Geomorphology, landuse, impact and rehabilitation. *Land Degrad. Dev.* **2004**, *15*, 115–121. [CrossRef]

28. LaChun, W.; YunLiang, S.H.I. Formation process and rational use of water resources and transform of rainfall, surface water and underground water in karst mountainous area in southwest China. *Sci. Geogr. Sin.* **2006**, *26*, 173–178. (In Chinese)
29. Huang, Q.; Cai, Y.; Xing, X. Rocky desertification, antidesertification, and sustainable development in the karst mountain region of southwest China. *Ambio* **2008**, *37*, 390–392. [CrossRef] [PubMed]
30. Qin, X.; Jiang, Z. Situation and comprehensive treatment strategy of drought in karst mountain areas of southwest China. *Adv. Res. Aquat. Environ.* **2011**, *1*, 383–389.
31. Bertrand, C.; Guglielmi, Y.; Denimal, S.; Mudry, J.; Deveze, G.; Carry, N. Hydrochemical response of a fractured carbonate aquifer to stress variations: Application to leakage detection of the Vouglans arch dam lake (Jura, France). *Environ. Earth Sci.* **2015**, *74*, 7671–7683. [CrossRef]
32. Stevanovic, Z.; Milanovic, P. Engineering challenges in karst. *Acta Carsol.* **2015**, *44*, 381–399. [CrossRef]
33. Zhu, S.; Zhang, J.; Wu, K.; Li, A.; Che, J. Device of purifying storage drinking water in rural karst engineering water shortage area. *J. Yangtze River Sci. Res. Inst.* **2013**, *30*, 20–23, 27. (In Chinese)
34. Zhu, W.; Li, P.; He, W.; Zhang, Y.; Li, H. Solutions and major scientific problem son engineer-ing water shortage in karst mountain area of Guizhou. *Guizhou Sci.* **2006**, *24*, 2–7. (In Chinese)
35. Parise, M.; Closson, D.; Gutierrez, F.; Stevanovic, Z. Anticipating and managing engineering problems in the complex karst environment. *Environ. Earth Sci.* **2015**, *74*, 7823–7835. [CrossRef]
36. Lu, Y.R.; Liu, Q.; Zhang, F.E. Environmental characteristics of karst in China and their effect on engineering. *Carbonates Evaporites* **2013**, *28*, 251–258. [CrossRef]
37. Mohammadi, Z.; Raeisi, E.; Bakalowicz, M. Method of leakage study at the karst dam site. A case study: Khersan 3 Dam, Iran. *Environ. Geol.* **2007**, *52*, 1053–1065. [CrossRef]
38. Su, W.C. Summary on ecological water requirement in karst mountain region of southwest China. *Guizhou Sci.* **2006**, *24*, 14–19. (In Chinese)
39. Li, A.D.; Yu, L.F.; Wei, X.L. The estmi ation on ecologicalwater requirement of forestland under differentmulching plantations in typicalkarst area. *J. Nanjing For. Univ. Nat. Sci. Ed.* **2011**, *35*, 57–61. (In Chinese)
40. Yang, S.T.; Wang, Y.J.; Lu, T.; Liu, R.L. Research on ecological water requirement quota of vegetation of karst areas—With a special reference to the middle of Guizhou. *Mod. Geogr. Sci. Soc. Econ. Guizhou* **2009**, *3*, 46–53. (In Chinese)
41. Zuo, T.; Diao, C.; Shi, K.; Sun, X.; Guan, D. Evaluation on ecological carrying capacity of epikarst dualistic water resources based on matter element analysis. *Acta Sci. Circumstantiae* **2014**, *34*, 1316–1323.
42. Song, W.-Z.; Yuan, Y.; Jiang, Y.-Z.; Lei, X.-H.; Shu, D.-C. Rule-based water resource allocation in the central Guizhou Province, China. *Ecol. Eng.* **2016**, *87*, 194–202. [CrossRef]
43. Wang, G.P. Study on afforestation tree species selection for rocky desertification restoration in Guiyang. *For. Sci. Technol.* **2012**, *37*, 37–41. (In Chinese)
44. Liu, Y.; Huang, X.; Yang, H.; Zhong, T. Environmental effects of land-use/cover change caused by urbanization and policies in southwest China karst area—A case study of Guiyang. *Habitat Int.* **2014**, *44*, 339–348. [CrossRef]
45. Gao, X.L.; Peng, S.Z.; Wang, W.G.; Xu, J.Z.; Yang, S.H. Spatial and temporal distribution characteristics of reference evapotranspiration trends in karst area: A case study in Guizhou Province, China. *Meteorol. Atmos. Phys.* **2016**, *128*, 677–688. [CrossRef]
46. Yang, P.; Tang, Y.Q.; Zhou, N.Q.; Wang, J.X.; She, T.Y.; Zhang, X.H. Characteristics of red clay creep in karst caves and loss leakage of soil in the karst rocky desertification area of Puding County, Guizhou, China. *Environ. Earth Sci.* **2011**, *63*, 543–549. [CrossRef]
47. Legrand, H.E. Hydrological and ecological problems of karst regions. *Science* **1973**, *179*, 859–864. [CrossRef] [PubMed]
48. Meng, J. The summary analysis on optimal allocation of Guiyang City's water resource. *Heilongjiang Sci. Technol. Water Conserv.* **2013**, *41*, 190–195. (In Chinese)
49. Bormann, H. Sensitivity of a soil-vegetation-atmosphere-transfer scheme to input data resolution and data classification. *J. Hydrol.* **2008**, *351*, 154–169. [CrossRef]
50. Yang, S.T.; Wang, Z.W.; Zhao, C.S.; Cai, M.Y. *Digital Experiment for Romote Sensing Application in Hydrology-Ecohat Handbook*; China Science Press: Beijing, China, 2015; pp. 115–137. (In Chinese)

51. Advanced Spaceborne Theemal Emissionand Reflection Radiometer Global Digital Elevation Model Net. Available online: http://www.Gisat.Cz/content/en/products/digital-elevation-model/aster-gdem (accessed on 21 March 2015).
52. The Portal of Chinese Science and Technology Resource Net. Available online: http://www.escience.gov.cn/default.jsp (accessed on 18 April 2015).
53. Nasa's Earch Observing System Data and Information System Net. Available online: http://ladsweb.nascom.nasa.gov/data/search.html (accessed on 30 March 2015).
54. Kang, S.Z.; Zhang, F.C.; Zhang, J.H. A simulation model of water dynamics in winter wheat field and its application in a semiarid region. *Agric. Water Manag.* **2001**, *49*, 115–129. [CrossRef]
55. Konrad, W.; Roth-Nebelsick, A. Integrating plant gas exchange, soil, and hydrological parameters in an analytical model: Potential use and limitations. *Vadose Zone J.* **2011**, *10*, 1196–1204. [CrossRef]
56. Amabile, A.; Balzano, B.; Caruso, M.; Tarantino, A. *A Conceptual Model for Water-Limited Evapotranspiration Taking into Account Root Depth, Root Density, and Vulnerability to Xylem Cavitation*; CRC Press-Taylor & Francis Group: Boca Raton, FL, USA, 2014; pp. 1047–1052.
57. Manzoni, S.; Vico, G.; Porporato, A.; Katul, G. Biological constraints on water transport in the soil-plant-atmosphere system. *Adv. Water Resour.* **2013**, *51*, 292–304. [CrossRef]
58. Chen, J.Y.; Liu, C.M.; Wu, K. Evapotranspiration of soil-plant-atmospheric continuum—A simulation study with lysimeter. *Chin. J. Appl. Ecol.* **1999**, *10*, 45–48.
59. Coelho, M.B.; Villalobos, F.J.; Mateos, L. Modeling root growth and the soil-plant-atmosphere continuum of cotton crops. *Agric. Water Manag.* **2003**, *60*, 99–118. [CrossRef]
60. Feddes, R.A.; Roats, P.A.C. *Parameterizing the Soil-Water-Plant Root System*; Wageningen UR: Wageningen, The Netherlands, 2004; Volume 6, pp. 95–141.
61. Wang, P.; Yamanaka, T.; Li, X.-Y.; Wei, Z. Partitioning evapotranspiration in a temperate grassland ecosystem: Numerical modeling with isotopic tracers. *Agric. For. Meteorol.* **2015**, *208*, 16–31. [CrossRef]
62. Gao, J.; Wu, S.; Dai, E.; Hou, W. The progresses and prospects of research on water and heat balance at land surface in the karst region of southwest China. *Adv. Earth Sci.* **2015**, *30*, 647–653.
63. Yujuan, W.; Di, D.U.; Shengtian, Y.; Tao, L.U.; Ruilu, L. Consumption of green water resources in typical karst areaa case study in Longli, Guizhou. *Carsol. Sin.* **2008**, *27*, 340–346. (In Chinese)
64. Yang, S.T. The research on utilization of green water in karst area. In *The Progress of Hydrological Science Innovation (Composite)*; China Science Press: Beijing, China, 2014; pp. 100–106. (In Chinese)
65. Gao, J.B.; Xue, Y.K.; Wu, S.H. Potential impacts on regional climate due to land degradation in the Guizhou Karst Plateau of China. *Environ. Res. Lett.* **2013**, *8*. [CrossRef]
66. Li, Z.X.; Feng, Q.; Wei, L.; Wang, T.T.; Gao, Y.; Wang, Y.M.; Cheng, A.F.; Li, J.G.; Liu, L. Spatial and temporal trend of potential evapotranspiration and related driving forces in southwestern China, during 1961–2009. *Quat. Int.* **2014**, *336*, 127–144.
67. Liu, C.M.; Yang, S.T.; Wen, Z.Q.; Wang, X.L.; Wang, Y.J.; Li, Q.; Sheng, H.R. Development of ecohydrological assessment tool and its application. *Sci. China Ser. E Technol. Sci.* **2009**, *52*, 1947–1957. [CrossRef]
68. Dong, G.T.; Yang, S.T.; Gao, Y.F.; Bai, J.; Wang, X.L.; Zheng, D.H. Spatial evaluation of phosphorus retention in riparian zones using remote sensing data. *Environ. Earth Sci.* **2014**, *72*, 1643–1657. [CrossRef]
69. Priestley, C.H.B.; Taylor, R.J. On the assessment of surface heat flux and evaporation using large-scale parameters. *Mon. Weather Rev.* **1972**, *100*, 81–92. [CrossRef]
70. Zhao, L.L.; Wang, Z.G.; Xia, J.; Chen, X.; Qin, N. Improved priestley-taylor method and its application in complementary relationship evapotranspiration model. *Prog. Geogr.* **2011**, *30*, 805–810. (In Chinese)
71. Clulow, A.D.; Everson, C.S.; Mengistu, M.G.; Price, J.S.; Nickless, A.; Jewitt, G.P.W. Extending periodic eddy covariance latent heat fluxes through tree sap-flow measurements to estimate long-term total evaporation in a peat swamp forest. *Hydrol. Earth Syst. Sci.* **2015**, *19*, 2513–2534. [CrossRef]
72. Ma, N.; Zhang, Y.S.; Szilagyi, J.; Guo, Y.H.; Zhai, J.Q.; Gao, H.F. Evaluating the complementary relationship of evapotranspiration in the alpine steppe of the Tibetan Plateau. *Water Resour. Res.* **2015**, *51*, 1069–1083. [CrossRef]
73. Barella-Ortiz, A.; Polcher, J.; Tuzet, A.; Laval, K. Potential evaporation estimation through an unstressed surface-energy balance and its sensitivity to climate change. *Hydrol. Earth Syst. Sci.* **2013**, *17*, 4625–4639. [CrossRef]
74. Aston, A.R. Rainfall interception by eight small tress. *J. Hydrol.* **1979**, *42*, 383–396. [CrossRef]

75. Li, B.G.; Gong, Y.S.; Zuo, Q. *Farmland Soil Water Dynamic Model and Its Application*; Science Press: Beijing, China, 2000. (In Chinese)
76. Kerkides, P.; Kargas, G.; Argyrokastritis, I. The effect of different methods used for hysteretic K(H) determination on the infiltration simulations. *Irrig. Drain.* **2006**, *55*, 403–418. [CrossRef]
77. The Climate Data for 2013. Available online: http://cyfd.cnki.com.cn/Article/N2016010099000017.htm (accessed on 2 December 2016).
78. Zhang, X.; Xue, J.H.; Haibara, K.; Xu, X.T.; Tian, Y.; Toda, H.; Liu, Y.H. Nutrient dynamics and hydrological process of karst forests in mountainous area of central Guizhou Province, China. *Acta Phytoecol. Sin.* **2007**, *31*, 757–768. (In Chinese)
79. Zhang, Z.; Chen, X.; Shi, P.; Wei, L. Distributed hydrological model and eco-hydrological effect of vegetation in karst watershed. *Adv. Water Sci.* **2009**, *20*, 806–811. (In Chinese)
80. The Information of "Guiyang Water Resources Bulletin" for 2013. Available online: http://swglj.gygov.gov.cn/art/2014/9/12/art_30889_1047379.html (accessed on 2 December 2016).
81. Tennant, D.L. Instream flow regimens for fish, wildlife, recreation and related environmental resources. *Fisheries* **1976**, *1*, 6–10. [CrossRef]
82. Lin, L.; Jiajun, H.; Jianlu, Y. Neural network simulation of water and soil conservation benefit from changing of slope fields into terrace with stone bank in the karst mountains. *Syst. Sci. Compr. Stud. Agric.* **2006**, *22*, 288–291. (In Chinese)
83. Chen, S.Z.; Zhou, Z.F.; Yan, L.H. Influence of human inetrvention on ecosystem health in the karst rock desertification controlling process. *Res. Soil Water Conserv.* **2016**, *23*, 213–219. (In Chinese)
84. Luo, L.; Hu, J.J.; Yao, J.L. Analysis on benefits of water and soil conservation and increasing grain yield from the terrace on rocky desertification slopes in karst mountains. *J. Sediment Res.* **2007**, *6*, 8–13. (In Chinese)